Article

Amino-Substituted 3-Aryl- and 3-Heteroarylquinolines as Potential Antileishmanial Agents

Jared T. Hammill,* Vitaliy M. Sviripa, Liliia M. Kril, Diana Ortiz, Corinne M. Fargo, Ho Shin Kim, Yizhe Chen, Jonah Rector, Amy L. Rice, Malgorzata A. Domagalska, Kristin L. Begley, Chunming Liu, Vivek M. Rangnekar, Jean-Claude Dujardin, David S. Watt, Scott M. Landfear, and R. Kiplin Guy

Read Online

ACCESS | Metrics & More | Article Recommendations | Supporting Information

ABSTRACT: Leishmaniasis, a disease caused by protozoa of the *Leishmania* species, afflicts roughly 12 million individuals worldwide. Most existing drugs for leishmaniasis are toxic, expensive, difficult to administer, and subject to drug resistance. We report a new class of antileishmanial leads, the 3-arylquinolines, that potently block proliferation of the intramacrophage amastigote form of *Leishmania* parasites with good selectivity relative to the host macrophages. Early lead **34** was rapidly acting and possessed good potency against *L. mexicana* (EC_{50} = 120 nM), 30-fold selectivity for the parasite relative to the macrophage (EC_{50} = 3.7 μM), and also blocked proliferation of *Leishmania donovani* parasites resistant to antimonial drugs. Finally, another early lead, **27**, which exhibited reasonable in vivo tolerability, impaired disease progression during the dosing period in a murine model of cutaneous leishmaniasis. These results suggest that the arylquinolines provide a fruitful departure point for the development of new antileishmanial drugs.

Cpd 27
L. mexicana EC_{50} = 0.22 ± 0.14 μM
J774A.1 Macrophage EC_{50} = 3.7 ± 0.99 μM
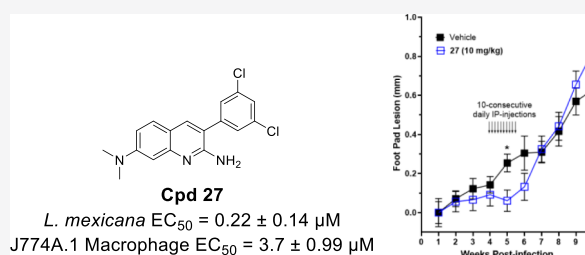
■ INTRODUCTION

Leishmaniasis is a neglected tropical disease whose causative organism possesses a complex life cycle that presents a difficult challenge for drug development.[1−4] Leishmaniases are caused by the protozoan parasites from the genus *Leishmania* carried between mammalian hosts by sandflies of the *Phlebotomus* and *Lutzomyia* genera. All *Leishmania* species have a digenetic life cycle that includes motile promastigotes that reside in the gut of the sand fly vector and nonmotile amastigotes that live in the phagolysosomal vesicles of mammalian host macrophages.[5] Leishmaniasis, endemic throughout the tropics, subtropics, and the Mediterranean basin, places an estimated 350 million people at risk and causes 1.5 million annual cases.[3,6−8] Leishmaniasis presents with a spectrum of symptoms and the WHO characterizes infections into three broad categories: the self-healing but disfiguring cutaneous leishmaniasis;[9] disfiguring mucocutaneous leishmaniasis;[10] and potentially fatal visceral leishmaniasis (VL).[11] In visceral disease, the parasites attack the patient's internal organs including the liver, spleen, and bone marrow. The annual morbidity of VL ranges as high as 100,000 people per year and more than 90% of cases occur in India, Bangladesh, Sudan, Ethiopia, and Brazil. Even when treated, VL has a mortality estimated at 10 to 20%.[7,12] If left untreated, the mortality rate of VL approaches 95%.[6]

The treatment of leishmaniasis depends on several factors including the type of disease, concomitant pathologies, parasite species, and the geographic location.[1,6,7,13,14] Current anti-leishmanial drugs include the antimonides[15] (e.g., sodium stibogluconate and meglumine antimonate), the bisamidines[16] (e.g., pentamidine), liposomal amphotericin B,[17] paromomycin,[18] and miltefosine.[19−22] Ideal new drugs for leishmaniasis should be orally bioavailable, active against all relevant species and strains, highly effective, minimally toxic, and inexpensive.[23−26] Most current drug discovery efforts target either cutaneous[27] or visceral[28] disease and although existing medicines find widespread application in afflicted populations, none possess the desired properties.[6,8] Only miltefosine can be administered orally, the ideal route for countries with rural populations with limited health care access.[19] All current drugs require lengthy treatment courses, and most are poorly tolerated or outright toxic.[1,7,29] Finally, resistance to the first-line antimonial drugs is common and resistance is emerging for the other classes of drugs.[30,31] Compounding these challenges, the different species and strains of *Leishmania* parasites exhibit distinct pathologies and differential susceptibility to novel chemotherapeutics.[5] Therefore, we embarked on a drug discovery campaign focused on identifying novel early lead compounds for leishmaniasis possessing potential to be developed into an orally bioavailable and efficacious drug.[32]

We previously reported a phenotypic high-throughput screen to identify new antileishmanial leads.[24] We have also pursued target-based approaches and the presence of microtubule-interacting[33] and vimentin-like proteins[34] in *Leishmania* parasites prompted our examination of the vimentin-targeting 3-arylquinolines (**2**, Figure 1), which were previously pursued as
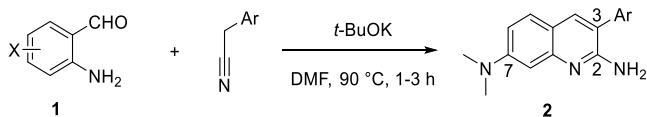

Figure 1. General synthetic route. A Friedländer condensation between aromatic *ortho*-aminobenzaldehydes **1** and aryl or heteroaryl acetonitriles in the presence of potassium tert-butoxide in *N,N*-dimethylformamide (90 °C for 1−3 h) afforded 3-arylquinolines **2** in good to excellent yields.

oncology leads.[35,36] We tested more than 100 existing 3-arylquinolines, at concentrations of 10 and 1 μM for 96 h, to determine if they affected proliferation of luciferase expressing *L. mexicana* intracellular amastigotes, a causative strain of cutaneous leishmaniasis, cultured in immortalized J774A.1 macrophages.[37] After lysis, host macrophage toxicity was assessed using the nucleic acid-binding dye SYBR Green I.[38] Inhibition of proliferation of nontransformed mammalian fibroblast cells (BJ fibroblast cells) was carried out in parallel (Supporting Information Table S1). After identifying hits, defined as > 70% inhibition at 1 μM, we carried out dose−response experiments (1 nM to 10 μM) to establish the potency of inhibiting proliferation (EC$_{50}$) of both the *L. mexicana* intracellular amastigotes and the host macrophages using the same test system. This study revealed several potent 3-arylquinolines (EC$_{50}$ < 250 nM) with significantly less potency against host macrophages (EC$_{50}$ > 3,000 nM), suggesting at least a 10-fold selectivity index (SI).[32] These data allowed us to define preliminary structure−activity relationships (SAR) within the series and 3-[3-(*N*-methylindolyl)-*N*^{7},*N*^{7}-dimethyl]-2,7-quinolinediamine (**34**) emerged as a potent, rapidly acting early lead also possessing significant potency against several patient-derived, antimony-resistant, strains of *Leishmania donovani*, a causative strain of VL. Next, we profiled selected analogs for in vitro ADME/Tox and in vivo pharmacokinetics in mice. Finally, we showed that compound **27**, which exhibited reasonable in vivo tolerability, significantly impaired disease progression in a murine model of cutaneous leishmaniasis. Together, these results suggest that the arylquinolines may provide a novel and promising starting point for the development of orally bioavailable antileishmanial drugs.

CHEMISTRY

Synthesis of 3-Arylquinolines. Friedländer condensation[39] between various *ortho*-aminobenzaldehydes (**1**) and either arylacetonitriles or heteroarylacetonitriles (Figure 1), using potassium *tert*-butoxide in *N,N*-dimethylformamide at 90 °C for 1−3 h, produced 3-arylquinolines in reasonable yields. The poorly stable 2-amino-4-(*N,N*-dimethylamino)-benzaldehyde was produced directly prior to use by the reduction of commercially available 4-(*N,N*-dimethylamino)-2-nitrobenzaldehyde with iron powder in hydrochloric acid. For the arylquinolines bearing C-7 heterocyclic groups, nucleophilic substitution reactions of 4-fluoro-2-nitrobenzaldehyde with either pyrrolidine, piperidine, and morpholine or *N*-methyl-

piperazine, followed by reduction with iron in hydrochloric acid, secured the required heterocyclic-substituted 2-aminobenzaldehydes. In all cases, the resulting free bases were treated with ethereal hydrochloric acid to afford more water-soluble salts than the corresponding free bases. All compounds utilized for biological assays had a structure confirmed by ^{1}H NMR, ^{13}C NMR, and mass spectrometry (MS) data and purity greater than 95% as confirmed by ultraperformance liquid chromatography (UPLC)−MS and/or combustion analyses.

RESULTS AND DISCUSSION

SARs: Initial Modifications. Our hit-to-lead strategy was to identify the pharmacophore and key structural drivers for potency (SAR), understand structural drivers for physiochemical properties such as solubility structure−property relationships (SPR), and evaluate metabolic and toxic liabilities inherent in the scaffolds. In exploring SAR, we adopted a strategy of systematically modifying the structural features embodied within **2** (Figure 2) in the following order: (1) the core
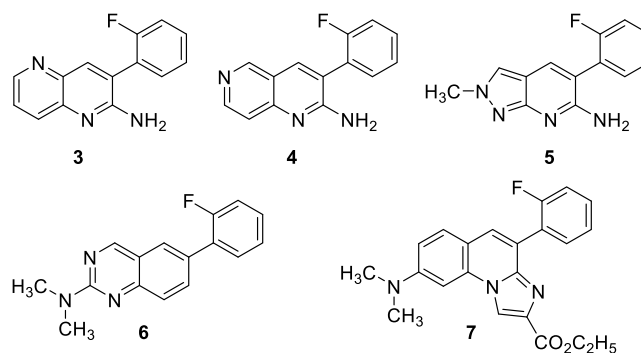

Figure 2. Modifications of the quinoline pharmacophore (Supporting Information Table S2).

quinoline system itself and (2) the pendent substituents at C-2, C-3, and C-7 positions on the quinoline ring. We tested the analogs to establish their growth inhibitory potency (EC$_{50}$) for both intracellular amastigotes and macrophages. To inspire confidence that efficacious plasma concentrations could be maintained without inducing gross toxicity in murine models, we initially sought to identify an arylquinoline with EC$_{50}$ < 250 nM for inhibiting proliferation of *L. mexicana* intracellular amastigotes and with a selectivity ratio against macrophages exceeding 25.[32]

We replaced the core quinoline ring system with other related heterocycles (Figure 2 and Supporting Information Table S2), beginning with the C-3 *ortho*-fluoroarylquinoline **16**, based on our previous work.[35,36] Our explorations (Figure 2 and Supporting Information Table S2) included introducing additional nitrogen atoms into the quinoline framework, as in 1,5-naphthyridine (**3**), 1,6-naphthyridine (**4**), and quinazoline (**5**); replacing the quinoline ring with another bicyclic heterocycle in 2-methyl-2*H*-pyrazolo[3,4-*b*]pyridine (**6**); and fusing an additional heterocyclic ring to the quinoline in imidazo[1,2-*a*]quinoline (**7**). Analogs **3**, **4**, and **5** exhibited little activity (≤25% inhibition at 10 μM). Analogs **6** and **7** possessed some activity but less potency than **2** (EC$_{50}$ > 1 μM). Therefore, we focused the remainder of our studies on the quinoline core.

SARs of 3-Arylquinolines: Modifications at C-2. Replacement of the C-2 amino group on the quinoline ring with a hydrogen (**8**), chloro (**9**), thiomethyl (**10**), morpholin-1-
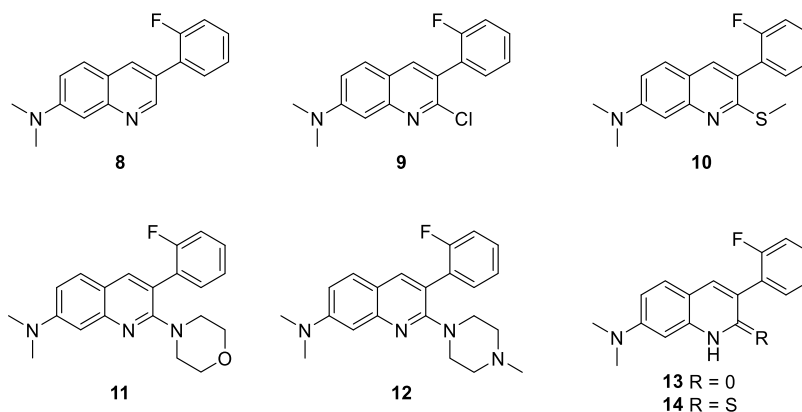
Figure 3. Modifications of the C-2 quinoline substituent (Supporting Information Table S2).
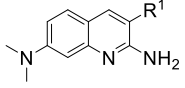
Table 1. Modifications of the C-3 Aryl Group[a]

No	R[1]	*L. mexicana* Amastigote EC$_{50}$ (µM)	J774A.1 Macrophage EC$_{50}$ (µM)	Ratio	No	R[1]	*L. mexicana* Amastigote EC$_{50}$ (µM)	J774A.1 Macrophage EC$_{50}$ (µM)	Ratio
15		0.63 ± 0.17	4.9 ± 0.90	8	22		0.40 ± 0.030	2.9 ± 0.070	7
16		0.45 ± 0.0	1.6 ± 0.0	4	23		0.35 ± 0.070	4.9 ± 3.8	14
17		0.28 ± 0.070	2.4 ± 0.75	8	24		0.76 ± 0.090	9.8 ± 4.5	13
18		0.61 ± 0.020	12 ± 5.1	20	25		0.50 ± 0.12	8.7 ± 1.2	17
19		0.33 ± 0.020	6.8 ± 1.6	21	26		0.34 ± 0.21	3.2 ± 1.8	9
20		0.30 ± 0.090	4.8 ± 0.14	16	27		0.22 ± 0.14	3.7 ± 0.99	17
21		0.36 ± 0.040	13 ± 3.5	35					

[a]Data represented as the mean of three replicates with errors reported as the standard deviation. Note: an error of 0.0 indicates identical values were obtained for each replicate.

yl (**11**), or 4-methylpiperazin-1-yl (**12**) group afforded weakly potent (EC$_{50}$ > 1 µM) inhibitors of amastigote proliferation (Figure 3 and Supporting Information Table S2). Likewise, replacement of the C-2 amino group in the quinoline ring with either a carbonyl (**13**) or thiocarbonyl (**14**) group, as in quinolin-2(1H)-ones or quinoline-2(1H)-thiones, respectively, also gave weakly potent analogs. From these data, a requirement for the hydrogen bond-donating and electron-rich amine at the C-2 position was identified.

SARs of 3-Arylquinolines: Modifications at C-3. Substitution of the C-3 aryl group with differentially substituted aryl groups and heteroaryl groups (Table 1) revealed minimal differences in potency (less than 2-fold) regardless of the electronic characteristics of the substituent. Likewise, we observed minimal changes in the SI (ratio of macrophage potency divided by intracellular amastigote potency) and none of the analogs met our target of 25-fold selectivity. Given the potential reduction of oxidative metabolism from halogenated

Table 2. Heterocyclic Modifications of the C-3 Aryl Group[a]

No	R[1]	*L. mexicana* Amastigote EC$_{50}$ (μM)	J774A.1 Macrophage EC$_{50}$ (μM)	Ratio	No	R[1]	*L. mexicana* Amastigote EC$_{50}$ (μM)	J774A.1 Macrophage EC$_{50}$ (μM)	Ratio
28		> 1	ND	ND	34		0.12 ± 0.090	3.7 ± 1.4	31
29		> 1	ND	ND	35		0.37 ± 0.22	14 ± 4.9	36
30		> 10	ND	ND	36		0.38 ± 0.030	5.1 ± 3.8	13
31		0.33 ± 0.030	2.2 ± 0.14	7	37		0.90 ± 0.84	4.9 ± 0.070	5
32		0.87 ± 0.17	16 ± 11	14	38		0.89 ± 0.18	10 ± 0.0	11
33		0.21 ± 0.020	4.4 ± 0.0	21					

[a]Data represented as the mean of three replicates with errors reported as the standard deviation. Note: an error of 0.0 indicates identical values were obtained for each replicate. ND = not determined.

analogs, we prioritized examining the chlorinated analogs that might afford a good balance between electronics and sterics without significantly compromising molecular weight. Subsequent studies showed that a chlorine atom could be placed in any position around the aryl ring without compromising potency. The *meta*-Cl (**21**) afforded the best SI (SI = 35). We selected 3-(3,5-dichlorophenyl)-N^7,N^7-dimethylquinoline-2,7-diamine (**27**), the first compound found with an EC$_{50}$ value below 250 nM and a good selectivity ratio (SI = 17) for further optimization.

Although reasonably potent and selective in cell-based assays, compound **27** was relatively hydrophobic (cLogP = 4.86), a finding that could limit its potential for in vivo studies.[40] Compounds with cLogP values >4 often exhibit rapid metabolic turnover, poor aqueous solubility, high plasma protein binding, and tissue accumulation.[41,42] They are also prone to receptor promiscuity and toxicity.[43] To address this issue, we tested whether the C-3 dichlorophenyl ring could be replaced by heterocycles while retaining potency and selectivity (Table 2). Smaller, five-membered heterocycles (**28**, **29**, and **30**) were significantly less potent than compounds **21** or **27**. Isosteric six-membered heterocycles retained or slightly improved potency. For example, the unsubstituted 2-pyridyl analog (**31**) was equipotent to **27** and predicted to be significantly less hydrophobic (cLogP = 2.82). More sterically encumbered bicyclic heterocycles were also well tolerated, with the methyl indole (**34**) proved to be potent and selective (EC$_{50}$ = 120 nM; SI = 30). This SAR suggested that the target possesses a

relatively deep and flexible hydrophobic pocket enveloping the C-3 substituent.

SARs of 3-Arylquinolines: Modifications at C-7. Replacement of the C-7 *N*,*N*-dimethylamino group allowed probing steric and electronic tolerances at that position while leaving the C-3 substituent fixed as either the 3,5-dicholoro or the *N*-methyl indole (Table 3). A secondary goal was to reduce crystallinity and hopefully improve kinetic aqueous solubility by incorporating a higher percentage of sp^3 hybridized carbons.[44,45] Our early pharmacophore studies (Figures 2 and 3) suggested the presence of a polar amino substituent at C-7 was critical for potency. Incorporation of either a pyrrolidine or piperidine afforded roughly equivalent potency. However, incorporation of the *N*-methylpiperazine or morpholine groups reduced potency 2- to 4-fold, suggesting the pocket was slightly less tolerant of distal polarity (Table 3). Overall, the range of potencies exhibited was narrow (<3-fold) and the trends exhibited were mirrored by both C-3 substituents. This led to the conclusion that the C-7 substituent could be chosen to improve physiochemcial properties without reducing potency and selectivity.

In Vitro Efficacy of Arylquinolines against Drug-Resistant *L. donovani* Strains. Arylquinoline **34**, possessing good intracellular amastigote activity (EC$_{50}$ = 120 nM) and a 30-fold SI, is a representative, early lead. We tested compound **34** against several patient-derived strains of *L. donovani*, a causative strain of VL: strain BPK282 that is antimonial-sensitive; strain BPK275 that is moderately antimonial-resistant; and strain

Table 3. Modification of the C-7 Group[a]

No	R[1]	R[2]	L. mexicana Amastigote EC$_{50}$ (µM)	J774A.1 Macrophage EC$_{50}$ (µM)	Ratio	No	R[1]	R[2]	L. mexicana Amastigote EC$_{50}$ (µM)	J774A.1 Macrophage EC$_{50}$ (µM)	Ratio
39			0.55 ± 0.15	3.7 ± 1.4	7	44			0.16 ± 0.28	4.1 ± 1.4	25
27			0.22 ± 0.14	3.7 ± 0.99	17	34			0.12 ± 0.090	3.7 ± 1.4	31
40			0.37 ± 0.060	1.4 ± 0.10	4	45			0.17 ± 0.040	0.44 ± 0.070	3
41			0.42 ± 0.090	6.8 ± 3.9	16	46			0.20 ± 0.090	0.56 ± 0.080	3
42			0.71 ± 0.33	ND	ND	47			0.64 ± 0.15	0.89 ± 0.10	1
43			0.53 ± 0.030	1.4 ± 0.15	4	48			0.62 ± 0.040	1.0 ± 0.25	2

[a]Data represented as the mean of three replicates with errors reported as the standard deviation. ND = not determined.

Table 4. Assessment of Potency (EC$_{50}$) Against Antimony-Resistant L. Donovani Parasites[a]

	antimony potassium tartrate	amphotericin B	miltefosine	arylquinoline 34
cell line	EC$_{50}$ (µM)	EC$_{50}$ (µM)	EC$_{50}$ (µM)	EC$_{50}$ (µM)
L. donovani **BPK282**	9.5 ± 5.4*	0.030 ± 0.026	6.2 ± 0.49	0.86 ± 0.25
L. donovani BPK275	18 ± 11*	0.027 ± 0.021	12 ± 2.1	0.71 ± 0.27
L. donovani **BPK173**	350 ± 240*	0.023 ± 0.017	16 ± 0.71	0.66 ± 0.28
L. mexicana	1.2 ± 0.53	0.23 ± 0.14	2.8 ± 1.2	0.12 ± 0.090

[a]Asterisks represent dose−response curves that are significantly different from each other for the three BPK lines, as determined using the sequential sum of squares F-test. Data represented as the mean of three replicates with errors reported as the standard deviation (Supporting Information Figure S1).

BPK173 that is highly antimonial-resistant.[30] Arylquinoline 34 retained activity against all resistant strains (Table 4 and Supporting Information Figure S1). Therefore, 34 is active against one of the causative strains of VL and does not appear to be subject to cross-resistance to antimony-based drugs.

Time of Effect Experiments. A metric for assessing the in vitro efficacy of antiparasitic compounds is to measure how quickly parasite numbers decline after drug treatment.[32] Rapidly acting drugs have the potential to relieve symptoms quickly and minimize the time-window for resistant parasite selection. To determine the time necessary to inhibit parasite growth, we exposed L. mexicana intracellular amastigotes to a range of concentrations of arylquinoline 34 for varying lengths of time (0.5, 2, 8.5, 24, 48, 72, and 96 h, Figure 4). Arylquinoline 34 rapidly inhibited the growth of intracellular amastigotes with an EC$_{50}$ of 1.0 µM after 0.5 h of incubation and appeared to approach its maximum effect by roughly 24 h of drug exposure.
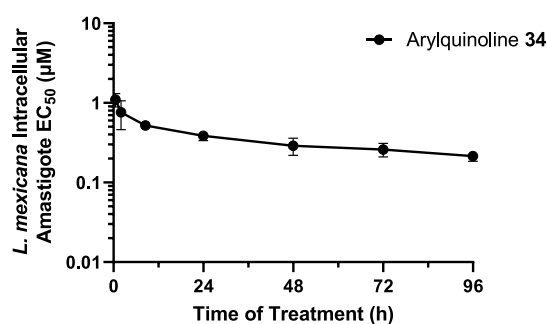

Figure 4. In vitro time of effect profiling of arylquinoline 34. Time-dependent EC$_{50}$ values were determined by exposing L. mexicana intracellular amastigotes to a range of concentrations of arylquinoline 34 for varying lengths of time (0.5, 2, 8.5, 24, 48, 72, and 96 h). Data represented as the mean of four replicates with errors reported as the standard deviation.

Table 5. Mouse Microsomal Stability Studies with Selected Arylquinolines[a]

No	R^1	R^2	Microsomal Half-life (h)	Microsomal Clearance CL_{int} (mL/min/kg)	No	R^1	R^2	Microsomal Half-life (h)	Microsomal Clearance CL_{int} (mL/min/kg)
15		phenyl	< 0.1	> 500	37		benzothiazole	0.20 ± 0.020	280 ± 6.2
16		2-F-phenyl	< 0.1	> 500	39		3,5-diCl-phenyl	> 4	< 10
17		2-Cl-phenyl	0.13 ± 0.010	420 ± 31	27		3,5-diCl-phenyl	0.17 ± 0.020	210 ± 1.9
22		4-Cl-phenyl	0.18 ± 0.020	290 ± 36	40		3,5-diCl-phenyl	0.20 ± 0.020	320 ± 46
23		2,3-diCl-phenyl	0.15 ± 0.010	360 ± 31	41		3,5-diCl-phenyl	0.10 ± 0.020	460 ± 1.0
24		2,5-diCl-phenyl	< 0.1	> 500	44		indole	1.3 ± 0.26	41 ± 8.0
31		pyridine	< 0.1	> 500	34		indole	0.26 ± 0.010	210 ± 9.9
33		4-phenylthiazole	0.31 ± 0.020	170 ± 8.5	45		indole	< 0.1	> 500
38		isopropylbenzoxazole	1.3 ± 0.11	43 ± 3.9	46		indole	0.80 ± 0.030	95 ± 4.2

[a]Data represented as the mean of two replicates with errors reported as the standard deviation.
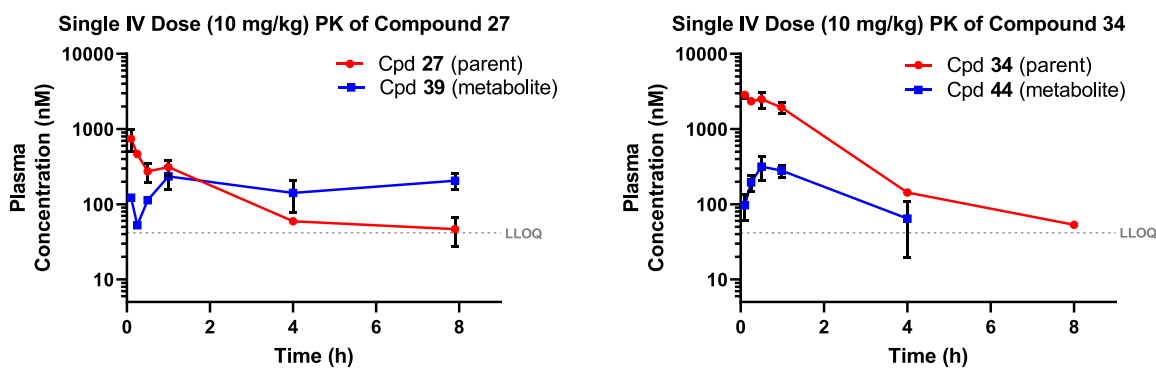

Figure 5. In vivo pharmacokinetic profiling of arylquinolines **27** and **34**. Murine pharmacokinetic studies for arylquinolines delivered intravenously at 10 mg/kg.

Mouse Liver Microsomal Metabolism. In order to finalize the selection of an early lead compound for in vivo studies, we characterized the metabolic stability of **34** and several related compounds using in vitro murine liver microsomes. These studies revealed that most analogs were rapidly metabolized (half-life, $t_{1/2}$ < 15 min, Table 5). In order to understand the

Table 6. Pharmacokinetic Parameters for Compounds 27 and 34 Based on Intravenous, Oral, and IP Administration in Mice[a]

arylquinoline	dose (mg/kg)	$t_{1/2}$ (h)	C_{max} (μM)	t_{max} (h)	AUC (μM*h)	CL (L/h/kg)	V_d (L/kg)
27 (IV)	10	2.32	0.741	NA	3.91	7.7	25.9
34 (IV)	10	1.29	2.84	NA	5.95	5.31	9.88
34 (PO)	10	0.68	1.00	0.1	0.921	33.4	33.6
34 (IP)	10	0.88	3.17	0.1	3.81	7.92	10.1

[a]Legend: $t_{1/2}$ is the compound half-life in plasma; C_{max} is the maximum concentration; t_{max} is the time the compound takes to achieve the maximum plasma concentration; AUC is the area-under-the-curve; CL is the clearance; and V_d is the volume of distribution at the steady state for IV, and apparent volume of distribution for other routes.

primary sites of metabolism, we carried out UPLC−MS analysis of compounds **27** and **34** after microsomal incubation. These studies revealed that oxidative demethylation of the C-7 *N,N*-dimethylamino group to the corresponding monomethyl counterparts was the major site of metabolism. Further exploration with other analogs suggested the monomethyl compounds (**39** and **44**) were the most stable, having $t_{1/2} > 1$ h.

In Vivo Pharmacokinetics. To evaluate the potential of the early lead arylquinolines (**27** and **34**) in vivo and begin to establish an in vitro to in vivo correlation, we performed preliminary single intravenous dose pharmacokinetic studies in mice to determine circulating plasma concentrations of both the parent (**27** and **34**) and monomethyl compounds (**39** and **44**). Following a single intravenous (IV) administration of arylquino-line **27** (10 mg/kg) to mice (Figure 5), the plasma concentration reached a peak (C_{max}) of 0.74 μM, had an elimination half-life ($t_{1/2}$) of 2.3 h, and an AUC of 3.91 μM*h (Table 6). Compound **27** concentrations in plasma remained above its in vitro EC_{50} of 0.22 μM for approximately 2 h. As the concentrations of the dimethyl amino (**27**) dwindled, the plasma concentration of the monomethyl metabolite (**39**) increased, suggesting it remained a primary metabolite in vivo and that the microsomal models were faithfully predicting metabolism. Following a single intravenous (IV) administration of arylquinoline **34** (10 mg/kg) in mice (Figure 5), the plasma concentration peaked (C_{max}) at 2.84 μM, the elimination half-life ($t_{1/2}$) was 1.29 h, and the AUC was 5.95 μM*h (Table 6). Compound **34** remained above its EC_{50} of 0.12 μM for approximately 4 h. Again, as concentrations of the dimethyl parent (**34**) decreased, the plasma concentration of the monomethyl metabolite (**44**) increased. However, the relatively lower exposure of the monomethyl metabolite **44** suggests other routes of metabolism are also at play.

Among the current standard of care agents for the treatment of leishmaniasis, only miltefosine is orally bioavailable. To begin to understand the bioavailability of the arylquinolines, we conducted single oral dose studies with compound **34** using a highly solubilizing formulation (10/10/40/39 EtOH/PG/PEG400/phosphate buffered saline (PBS) (pH 7.4) and 1% w/v HβCD). Following a single oral dose of **34** (10 mg/kg, Figure 5 and Table 6) to mice, compound **34** showed rapid absorption ($t_{max} \sim 0.1$ h) with a C_{max} of 1.0 μM, a $t_{1/2}$ of 0.68 h, and an AUC of 0.921 μM*h. The plasma concentration remained above the EC_{50} of 0.12 μM for about 2 h. The apparent oral bioavailability (15%) was lower than optimal and did not reach concentrations expected to deliver the desired efficacy. Therefore, intraperitoneal injection (IP) was also explored. IP injection achieved a much higher exposure than oral administration and C_{max} (3.17 μM) and overall AUC (3.81 μM*h) values were much closer to those observed after IV dosing.

Given the better exposures from the IP route than the oral route, we evaluated 10 sequential daily IP injections of **34** in a murine model. Unfortunately, daily IP administration of **34** in a 100% dimethyl sulfoxide (DMSO) solution led to significant adverse events including: rough hair, hunched posture, distended abdomen, lethargy, seizures, and bloody stool. These effects were not observed after repeated IP injection of compound **27**. Thus, the hydrochloride salt of **27** was chosen for in vivo efficacy testing. The improved water solubility of this salt permitted dosing as a solution of 50% PEG400 in isotonic PBS rather than dosing as a DMSO solution.

In Vivo Pharmacodynamics. Arylquinoline **27** was tested for efficacy using an in vivo footpad murine model of cutaneous leishmaniasis.[46] Briefly, the footpad of BALB/c mice was injected with 10^6 *L. mexicana* parasites on day zero. Four weeks after inoculation, a palpable lesion was observed, and drug treatment was initiated. Cohorts of five animals were treated either with arylquinoline **27** (10 mg/kg) for 10 consecutive days administered by IP injection (50% PEG400 in PBS$_{7.4}$), or with vehicle alone as a negative control. Lesion size (determined by caliper) was measured for six additional weeks postdrug treatment (Figure 6). For vehicle-treated mice, the lesions grew steadily for 10 weeks, at which time the mice were euthanized. During the administration period, arylquinoline **27** fully inhibited the progression of lesion size, maintaining dimensions matching those at the time of initial dosing (i.e., at
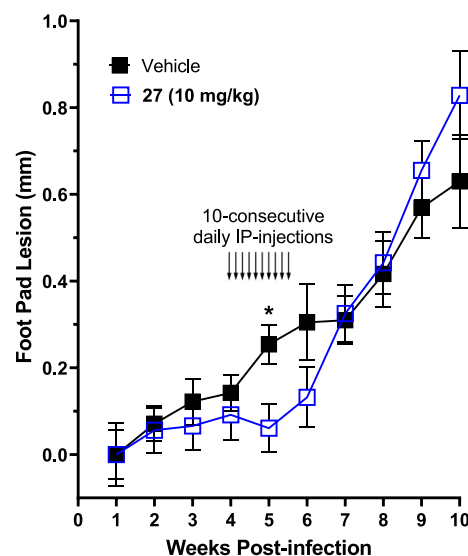

Figure 6. In vivo efficacy for controlling cutaneous lesion progression in the mouse. Mice (5 per cohort) were infected with *L. mexicana* promastigotes on day 0; by week 4 after infection, cutaneous lesions had grown to ~0.1 mm width. Vehicle or arylquinoline **27** (10 mg/kg) was delivered daily by IP injection for 10 consecutive days. Measurements are plotted as the mean ± standard deviation. *$p < 0.01$.

4 weeks postinjections with *L. mexicana*). However, after drug treatment was withdrawn, the footpad lesions began to increase in size, eventually growing to a size roughly equivalent to the size seen for vehicle treatment.

CONCLUSIONS

Leishmaniasis comprises of a spectrum of diseases with significant unmet clinical need and the development of novel therapeutics for leishmaniasis remains particularly challenging. The current target product profile for new antileishmanial drugs requires oral bioavailability, activity against drug-resistant strains, excellent potency, high efficacy, minimal toxicity, and low cost.[23] We investigated whether the 3-arylquinolines[36] could provide a new starting point for the development of antileishmanial drugs. We tested more than 100 arylquinoline analogs at 1 μM and 10 μM for their ability to block growth of intracellular amastigotes, the disease-causing stage of the *Leishmania* parasite. We determined growth inhibition potencies (EC_{50}) against both the amastigotes and the host macrophages in which they reside for the most active compounds. These studies revealed several 3-arylquinolines with potent ($EC_{50} <$ 250 nM) antileishmanial activity and weaker potency ($EC_{50} >$ 3,000 nM) against macrophages, giving at least a 10-fold SI.

Initial studies defining the pharmacophore involved large structural perturbations to the quinoline core and demonstrated that roughly isosteric 6,6- and 6,5- heteroaryl cores were significantly less potent (Figure 2). We systematically explored the substituents at C-2, C-3, and C-7 positions on the quinoline ring. The aryl substituent at the C-3 position apparently occupies a relatively deep and flexible hydrophobic pocket on the target that can accommodate a range of electron-donating and electron-withdrawing substituents and six-membered heterocycles (Tables 2 and 3). However, there is a requirement for a reasonable steric bulk because smaller, five-membered heterocycles were significantly less potent (Table 3).

Examining physiochemical characteristics and metabolic stability of a small number of analogs revealed the current generation of arylquinolines has a high cLogP (>5) and are rapidly cleared in microsomal models of oxidative metabolism ($Cl_{int} >$ 80 ml/min/kg) (Table 5). Metabolite identification studies after microsomal incubation revealed that a single demethylation of the *N,N*-dimethylamino group was the primary metabolic event. Fortuitously, the monomethyl analogs of **27** and **34** retained their parent's amastigote growth inhibition potency. To mitigate the metabolism of the labile *N,N*-dimethylamino substituent, we prepared a series of C-7 related compounds containing amines of varying basicity and steric bulk, while attempting to increase solubility by introducing nonplanar cyclic systems to confer flexibility and decrease the propensity to form crystal lattices (Table 3). These studies revealed that the *N,N*-dimethylamino group could be replaced by the piperidine or pyrrolidine with retention of potency but unfortunately without improved microsomal stability. Therefore, arylquinoline **34** was chosen as a representative early lead with promising rapid intracellular amastigote activity (EC_{50} = 120 nM) and a 30-fold selectivity over macrophage toxicity (EC_{50} = 3.7 μM). Compound **34** was also shown to retain potency in both moderately and significantly drug-resistant, patient-derived *L. donovani* parasites (Table 4), demonstrating activity against causative strains of both cutaneous and VL.

To establish an in vitro to in vivo correlation, we selected two potent analogs, **27** and **34**, for preliminary in vivo PK studies. A single low-dose (10 mg/kg) murine intravenous (IV) PK study

of either **27** or **34** showed no gross toxicity but revealed rapid clearance and the formation of significant quantities of the monomethyl metabolites (Figure 5). Complementary single oral dosing studies suggest **34** has poor bioavailability ($F <$ 20%). One explanation for the observed low bioavailability is that the compounds are rapidly metabolized by the liver during first-pass metabolism, effectively limiting the amount of drug that can reach systemic circulation. Although repeated IP injection of **34** proved toxic, delivery of **27** at 10 mg/kg IP daily for 10 days proved tolerable and led to partial control of an in vivo infection with *L. mexicana*. The sizes of cutaneous lesions, however, returned to those of untreated animals following cessation of treatment.

In conclusion, the 3-arylquinolines feature a compact size, good potency, a clear SAR, and synthetic accessibility that together with the reasonable murine exposure and partial control of disease progression exhibited by arylquinoline **27** suggest they can be considered viable early leads for leishmaniasis therapy. However, future studies must determine if the arylquinolines can mechanistically clear an infection or if the apparent stasis is a function of achieved compound concentrations. Future studies should also focus on understanding the mechanistic drivers of both amastigote growth inhibition and of the in vivo toxicity observed after repeated administration of **34**, suppressing oxidative metabolism using microsomal models, and improving physiochemical properties and in vivo pharmacokinetics and pharmacodynamics.

EXPERIMENTAL SECTION

Chemistry. *General Chemistry.* Chemicals were purchased from Sigma-Aldrich (St. Louis, MO) or Fisher Scientific (Pittsburgh, PA) unless otherwise noted or were synthesized according to literature procedures. Solvents were obtained from commercial vendors without further purification unless otherwise noted. Nuclear magnetic resonance spectra were obtained on Varian instruments (^{1}H, 400 or 500 MHz; ^{13}C, 100 or 126 Mz). Chemical shifts (δ) are reported in parts per million (ppm) with internal CHCl$_3$ (δ 7.26 ppm for ^{1}H and 77.0 ppm for ^{13}C), internal DMSO (δ 2.50 ppm for ^{1}H and 39.5 ppm for ^{13}C), or internal TMS (δ 0.0 ppm for ^{1}H and 0.0 ppm for ^{13}C) as the reference. ^{13}C NMR data are reported as follows: chemical shift, multiplicity (s = singlet, bs = broad singlet, d = doublet, t = triplet, q = quartet, p = pentet, sext = sextet, sep = septet, m = multiplet, dd = doublet of doublets, dt = doublet of triplets, td = triplet of doublets, and qd = quartet of doublets), coupling constant(s) (J) in Hertz (Hz), and integration. Low-resolution mass spectra were obtained using an Agilent 1100 (atmospheric pressure and chemical ionization) instrument. High-resolution mass data were obtained by direct infusion electrospray ionization MS using a LTQ-Orbitrap mass spectrometer coupled with a heated electrospray ionization (HESI-II) Probe (Thermo Fisher Scientific, Waltham, MA) and an FT analyzer at a resolution of 100,000. The reported *m/z* mass was a mean of 20 scans. Melting points were determined in open capillary tubes with a Buchi B-535 apparatus and are uncorrected. Compounds were purified by chromatography on preparative layer Merck silica gel F254 unless otherwise noted. Combustion analyses were conducted at Atlantic Microlabs (Norcross, GA). All compounds were characterized for structural assignments and purity by a combination of ^{1}H and ^{13}C NMR, MS data, and combustion analyses. All compounds utilized for biological assays had a confirmed structure and purity greater than 95%.

General Procedure for the Synthesis of Arylquinolines.[35,36] To a solution of 2.38 mmol (1.3 equiv) of the appropriate benzyl cyanide in 3 mL of anhydrous *N,N*-dimethylformamide at 0 °C was added 2.38 mmol (1.3 equiv) of potassium *tert*-butoxide. The mixture was stirred for 15 min, and 1.83 mmol of appropriate 2-aminobenzaldehyde dissolved in 1 mL of anhydrous *N,N*-dimethylformamide was added dropwise at 0 °C. The mixture was warmed to 25 °C and stirred for 3−4

h at 90 °C. After cooling, the mixture was quenched by pouring into water to afford a precipitate that was collected and purified by recrystallization and/or chromatography as noted for individual compounds described below.
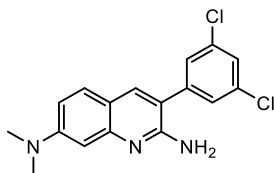
3-[3,5-Dichlorophenyl]-N[7],N[7]-dimethylquinoline-2,7-diamine (27). Purified by chromatography with methanol: dichloromethane (1:10) as the eluent three times: yield 88%, mp 169−171 °C. ^{1}H NMR, 400 MHz (DMSO-d_6): δ ppm 7.72 (s, 1H), 7.58 (t, J = 1.8 Hz, 1H), 7.52−7.49 (m, 3H), 6.86 (dd, J = 8.8 and 2.4 Hz, 1H), 6.59 (d, J = 2 Hz, 1H), 5.95 (s, 2H, NH$_2$), 3 (s, 6H). ^{13}C NMR, 100 MHz, (DMSO-d_6): δ ppm 151.5, 149.1, 142, 137.1, 134.3, 128.4, 127.5, 126.7, 117.3, 115.4, 111.3, 103.3, 40. HRMS (ESI) calcd for $C_{17}H_{16}{}^{35}Cl{}^{35}ClN_3$ [MH$^+$], 332.0716; found, 332.0708; calcd for $C_{17}H_{16}{}^{35}Cl{}^{37}ClN_3$ [MH$^+$], 334.0747; found, 332.0661; calcd for $C_{17}H_{16}{}^{37}Cl{}^{37}ClN_3$ [MH$^+$], 336.0629; found, 336.0657.
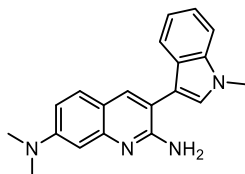
3-[3-(N-Methylindolyl)-N[7],N[7]-dimethyl]-2,7-quinolinediamine (34). Purified by chromatography using methanol: dichloromethane (1:10) as the eluent and recrystallized from acetonitrile: yield 45%, mp 152−155 °C. ^{1}H NMR, 400 MHz (DMSO-d_6): δ ppm 7.76 (s, 1H), 7.58 (s, 1H), 7.55 (d, J = 7.6, 1H), 7.52 (d, J = 8 Hz, 1H), 7.5 (d, J = 8.4 Hz, 1H), 7.23 (t, J = 8 Hz, 1H), 7.1 (t, J = 8 Hz, 1H), 6.86 (dd, J = 8.8 and 2.4 Hz, 1H), 6.65 (d, J = 2.4 Hz, 1H), 5.84 (s, 2H, NH$_2$), 3.86 (s, 3H), 3 (s, 6H). ^{13}C NMR, 100 MHz, (DMSO-d_6): δ ppm 156.6, 151, 148, 136.8, 135.7, 128.7, 127.8, 126.5, 121.6, 119.4, 119.3, 115.8, 113.4, 111, 110.5, 110.1, 103.9, 40.3, 32.6. HRMS (ESI) calcd for $C_{20}H_{21}N_4$ [MH$^+$], 317.1761; found: 317.1748. Anal. Calcd for $C_{20}H_{20}N_4$: C, 75.92; H, 6.37. Found: C, 75.77; H, 6.26.

Biology. *Assays for Growth Inhibition of Leishmania Intracellular Amastigotes.* RLuc *L. mexicana* and Hluc *L. donovani-BPK* stationary phase promastigotes were used to infect J774A.1 macrophages at a multiplicity of infection of 10:1 and 5:1, respectively. After overnight 16 h incubation, infected macrophages were washed three times in PBS to remove extracellular promastigotes and transferred to 96-well plates at a seeding density of 1×10^4 parasites per well in 0.2 mL Minimal Essential Media (Gibco). Compounds (2 μL volumes in DMSO) were added to the parasites using serial 3-fold dilutions to cover a range of concentrations from about 10 μM to 1 nM. Cultures were incubated at 37 °C under a humidified 5% CO$_2$ atmosphere for 96 h for RLuc *L. mexicana* parasites or 72 h for *L. donovani* Hluc-BPK cells, unless otherwise noted for time of effect studies. Growth of intracellular amastigotes was measured using the *Renilla* luciferase assay system (Promega), as detailed previously[37] for RLuc parasites and ONE-Glo (Promega) for Hluc-BPK cells.

Cytotoxicity of compounds to J774.A1 macrophages was quantified separately; 10 μL of 100 X stock SYBR Green I (Sigma-Aldrich) in 10% Triton in PBS was added to 100 μL of lysed cells and fluorescence measured (Ex 497 nm; Em 520 nm) after 1 h incubation in the dark using a Wallac 1420 Victor2 Microplate Reader. Data were log transformed and EC$_{50}$ values were determined using GraphPad Prism 8 (GraphPad Software). In the absence of growth inhibitors or DMSO, the macrophages increased in number ~6-fold over 96 h in Minimum Essential Medium, employed for both macrophage infections and the toxicity assays.

Animal Studies Statement. All animal studies carried out to support this work were executed under approved protocols governed by the respective Institutional Animal Care and Use Committees.

Efficacy Studies Using the Murine Model of Cutaneous Leishmaniasis. Female BALB/c mice (~20 g) were injected in one hind foot pad with 1×10^6 stationary phase promastigotes suspended in 25 μL of PBS. Four weeks after infection, when a small cutaneous lesion was visible in the injected footpad, cohorts of five mice were treated with either compound or vehicle alone (90 μL), delivered daily for 10 consecutive days by IP injection using a 20-gauge × 30 mm disposable plastic needle. Vehicle consisted of 50% PEG400 in isotonic PBS. The width of the footpad (top to bottom) was measured with calipers before injection of parasites (day 0) and weekly from weeks 4−10. The width of the uninfected contralateral footpad was also measured each week, and its width was subtracted from that of the infected footpad to determine the lesion size.

■ ASSOCIATED CONTENT

ⓢ Supporting Information

The Supporting Information is available free of charge at https://pubs.acs.org/doi/10.1021/acs.jmedchem.1c00813.

> Molecular formula strings and growth inhibition data for *L. mexicana* intracellular amastigotes, J774A.1 macrophages, and normal fibroblasts (BJ) (CSV)

> NMR (^{1}H & ^{13}C) characterization, melting point, mass spectra, and elemental analysis data and experimental details regarding biological and in vivo studies (PDF)

■ AUTHOR INFORMATION

Corresponding Author

Jared T. Hammill — *Department of Pharmaceutical Sciences, College of Pharmacy, University of Kentucky, Lexington, Kentucky 40536-0509, United States;* ⓞ orcid.org/0000-0002-9463-0526; Phone: 859-257-0484; Email: Jared.Hammill@uky.edu

Authors

Vitaliy M. Sviripa — *Department of Pharmaceutical Sciences, College of Pharmacy, University of Kentucky, Lexington, Kentucky 40536-0509, United States; Center for Pharmaceutical Research and Innovation, College of Pharmacy, University of Kentucky, Lexington, Kentucky 40536-0596, United States; Lucille Parker Markey Cancer Center, University of Kentucky, Lexington, Kentucky 40536-0093, United States;* ⓞ orcid.org/0000-0002-7272-373X

Liliia M. Kril — *Center for Pharmaceutical Research and Innovation, College of Pharmacy, University of Kentucky, Lexington, Kentucky 40536-0596, United States; Department of Molecular and Cellular Biochemistry, College of Medicine, University of Kentucky, Lexington, Kentucky 40536-0509, United States*

Diana Ortiz — *Department of Molecular Microbiology and Immunology, Oregon Health and Science University, Portland, Oregon 97239, United States*

Corinne M. Fargo — *Department of Molecular Microbiology and Immunology, Oregon Health and Science University, Portland, Oregon 97239, United States*

Ho Shin Kim — *Department of Pharmaceutical Sciences, College of Pharmacy, University of Kentucky, Lexington, Kentucky 40536-0509, United States*

Yizhe Chen — *Department of Pharmaceutical Sciences, College of Pharmacy, University of Kentucky, Lexington, Kentucky 40536-0509, United States*

Jonah Rector — *Department of Pharmaceutical Sciences, College of Pharmacy, University of Kentucky, Lexington, Kentucky 40536-0509, United States*

Amy L. Rice − *Department of Pharmaceutical Sciences, College of Pharmacy, University of Kentucky, Lexington, Kentucky 40536-0509, United States;* ⊙ orcid.org/0000-0001-7398-9022

Malgorzata A. Domagalska − *Department of Biomedical Sciences, Institute of Tropical Medicine, Antwerpen 2000, Belgium*

Kristin L. Begley − *Center for Pharmaceutical Research and Innovation, College of Pharmacy, University of Kentucky, Lexington, Kentucky 40536-0596, United States; Department of Molecular and Cellular Biochemistry, College of Medicine, University of Kentucky, Lexington, Kentucky 40536-0509, United States*

Chunming Liu − *Lucille Parker Markey Cancer Center, University of Kentucky, Lexington, Kentucky 40536-0093, United States; Department of Molecular and Cellular Biochemistry, College of Medicine, University of Kentucky, Lexington, Kentucky 40536-0509, United States*

Vivek M. Rangnekar − *Lucille Parker Markey Cancer Center, University of Kentucky, Lexington, Kentucky 40536-0093, United States; Department of Radiation Medicine, College of Medicine, University of Kentucky, Lexington, Kentucky 40506-9983, United States; Graduate Center for Toxicology, College of Medicine, University of Kentucky, Lexington, Kentucky 40536-0305, United States*

Jean-Claude Dujardin − *Department of Biomedical Sciences, Institute of Tropical Medicine, Antwerpen 2000, Belgium*

David S. Watt − *Department of Pharmaceutical Sciences, College of Pharmacy and Department of Molecular and Cellular Biochemistry, College of Medicine, University of Kentucky, Lexington, Kentucky 40536-0509, United States; Center for Pharmaceutical Research and Innovation, College of Pharmacy, University of Kentucky, Lexington, Kentucky 40536-0596, United States; Lucille Parker Markey Cancer Center, University of Kentucky, Lexington, Kentucky 40536-0093, United States*

Scott M. Landfear − *Department of Molecular Microbiology and Immunology, Oregon Health and Science University, Portland, Oregon 97239, United States*

R. Kiplin Guy − *Department of Pharmaceutical Sciences, College of Pharmacy, University of Kentucky, Lexington, Kentucky 40536-0509, United States;* ⊙ orcid.org/0000-0002-9638-2060

Complete contact information is available at:
https://pubs.acs.org/10.1021/acs.jmedchem.1c00813

Author Contributions
All authors participated in writing and gave their approval to the final version of the manuscript.

Notes
The authors declare no competing financial interest.

ABBREVIATIONS

ADME, absorption, distribution, metabolism, and excretion; UPLC, ultraperformance liquid chromatography; EC_{50}, half-maximal proliferation inhibitory concentration; WHO, World Health Organization; SAR, structure−activity relationship; SPR, structure−property relationships; VL, visceral leishmaniasis; CL, cutaneous leishmaniasis; SI, selectivity index; *L*, *Leishmania*; *t*-BuOK, Potassium *tert*-butoxide; DMF, *N,N*-dimethylformamide; DMSO, dimethyl sulfoxide; $t_{1/2}$, apparent compound half-life in plasma; C_{max}, maximum concentration; t_{max}, time the compound takes to achieve the maximum plasma concentration; AUC, area-under-the-curve; CL, cutaneous leishmaniasis; V_d, volume of distribution at steady state for IV and apparent volume of distribution for other routes

REFERENCES

(1) Mishra, J.; Saxena, A.; Singh, S. Chemotherapy of leishmaniasis: past, present and future. *Curr. Med. Chem.* **2007**, *14*, 1153.

(2) Steverding, D. The history of leishmaniasis. *Parasites Vectors* **2017**, *10*, 82.

(3) Akhoundi, M.; Kuhls, K.; Cannet, A.; Votýpka, J.; Marty, P.; Delaunay, P.; Sereno, D. A Historical Overview of the Classification, Evolution, and Dispersion of Leishmania Parasites and Sandflies. *PLoS Neglected Trop. Dis.* **2016**, *10*, No. e0004349.

(4) Lukes, J.; Mauricio, I. L.; Schonian, G.; Dujardin, J.-C.; Soteriadou, K.; Dedet, J.-P.; Kuhls, K.; Tintaya, K. W. Q.; Jirku, M.; Chocholova, E.; Haralambous, C.; Pratlong, F.; Obornik, M.; Horak, A.; Ayala, F. J.; Miles, M. A. Evolutionary and geographical history of the Leishmania donovani complex with a revision of current taxonomy. *Proc. Natl. Acad. Sci. U. S. A.* **2007**, *104*, 9375.

(5) Rodrigues, J. C. F.; Godinho, J. L. P.; de Souza, W. Biology of human pathogenic trypanosomatids: epidemiology, lifecycle and ultrastructure. *Subcell. Biochem.* **2014**, *74*, 1.

(6) Torres-Guerrero, E.; Quintanilla-Cedillo, M. R.; Ruiz-Esmenjaud, J.; Arenas, R. Leishmaniasis: a review. *F1000Research* **2017**, *6*, 750.

(7) Alves, F.; Bilbe, G.; Blesson, S.; Goyal, V.; Monnerat, S.; Mowbray, C.; Muthoni Ouattara, G.; Pécoul, B.; Rijal, S.; Rode, J.; Solomos, A.; Strub-Wourgaft, N.; Wasunna, M.; Wells, S.; Zijlstra, E. E.; Arana, B.; Alvar, J. Recent Development of Visceral Leishmaniasis Treatments: Successes, Pitfalls, and Perspectives. *Clin. Microbiol. Rev.* **2018**, *31*, No. e00048.

(8) Molyneux, D. H.; Savioli, L.; Engels, D. Neglected tropical diseases: progress towards addressing the chronic pandemic. *Lancet* **2017**, *389*, 312.

(9) Reithinger, R.; Dujardin, J.-C.; Louzir, H.; Pirmez, C.; Alexander, B.; Brooker, S. Cutaneous leishmaniasis. *Lancet Infect. Dis.* **2007**, *7*, 581.

(10) David, C. V.; Craft, N. Cutaneous and mucocutaneous leishmaniasis. *Dermatol. Ther.* **2009**, *22*, 491.

(11) Chappuis, F.; Sundar, S.; Hailu, A.; Ghalib, H.; Rijal, S.; Peeling, R. W.; Alvar, J.; Boelaert, M. Visceral leishmaniasis: what are the needs for diagnosis, treatment and control? *Nat. Rev. Microbiol.* **2007**, *5*, 873.

(12) Alvar, J.; Vélez, I. D.; Bern, C.; Herrero, M.; Desjeux, P.; Cano, J.; Jannin, J.; Boer, M. d.; Team, W. H. O. L. C. Leishmaniasis worldwide and global estimates of its incidence. *PloS One* **2012**, *7*, No. e35671.

(13) Thompson, A. M.; O'Connor, P. D.; Yardley, V.; Maes, L.; Launay, D.; Braillard, S.; Chatelain, E.; Wan, B.; Franzblau, S. G.; Ma, Z.; Cooper, C. B.; Denny, W. A. Novel Linker Variants of Antileishmanial/Antitubercular 7-Substituted 2-Nitroimidazooxazines Offer Enhanced Solubility. *ACS Med. Chem. Lett.* **2021**, *12*, 275.

(14) Sangshetti, J. N.; Kalam Khan, F. A.; Kulkarni, A. A.; Arote, R.; Patil, R. H. Antileishmanial drug discovery: comprehensive review of the last 10 years. *RSC Adv.* **2015**, *5*, 32376.

(15) Sundar, S.; Chakravarty, J. Antimony toxicity. *Int. Res. J. Publ. Environ. Health* **2010**, *7*, 4267.

(16) Yang, G.; Choi, G.; No, J. H. Antileishmanial Mechanism of Diamidines Involves Targeting Kinetoplasts. *Antimicrob. Agents Chemother.* **2016**, *60*, 6828.

(17) Sundar, S.; Jaya, J. Liposomal amphotericin B and leishmaniasis: dose and response. *J. Global Infect. Dis.* **2010**, *2*, 159.

(18) Sundar, S.; Chakravarty, J. Paromomycin in the treatment of leishmaniasis. *Expert Opin. Invest. Drugs* **2008**, *17*, 787.

(19) Croft, S. L.; Sundar, S.; Fairlamb, A. H. Drug resistance in leishmaniasis. *Clin. Microbiol. Rev.* **2006**, *19*, 111.

(20) Croft, S. L.; Engel, J. Miltefosine–discovery of the antileishmanial activity of phospholipid derivatives. *Trans. R. Soc. Trop. Med. Hyg.* **2006**, *100*, S4.

(21) Berman, J.; Bryceson, A. D. M.; Croft, S.; Engel, J.; Gutteridge, W.; Karbwang, J.; Sindermann, H.; Soto, J.; Sundar, S.; Urbina, J. A. Miltefosine: issues to be addressed in the future. *Trans. R. Soc. Trop. Med. Hyg.* **2006**, *100*, S41.

(22) Dorlo, T. P. C.; Balasegaram, M.; Beijnen, J. H.; de Vries, P. J. Miltefosine: a review of its pharmacology and therapeutic efficacy in the treatment of leishmaniasis. *J. Antimicrob. Chemother.* **2012**, *67*, 2576.

(23) Target product profile for cutaneous leishmaniasis: DNDi. https://dndi.org/diseases/cutaneous-leishmaniasis/target-product-profile/ (accessed March 21, 2021).

(24) Ortiz, D.; Guiguemde, W. A.; Hammill, J. T.; Carrillo, A. K.; Chen, Y.; Connelly, M.; Stalheim, K.; Elya, C.; Johnson, A.; Min, J.; Shelat, A.; Smithson, D. C.; Yang, L.; Zhu, F.; Guy, R. K.; Landfear, S. M. Discovery of novel, orally bioavailable, antileishmanial compounds using phenotypic screening. *PLoS Neglected Trop. Dis.* **2017**, *11*, No. e0006157.

(25) Alcântara, L. M.; Ferreira, T. C. S.; Gadelha, F. R.; Miguel, D. C. Challenges in drug discovery targeting TriTryp diseases with an emphasis on leishmaniasis. *Int. J. Parasitol.: Drugs Drug Resist.* **2018**, *8*, 430.

(26) Caridha, D.; Vesely, B.; van Bocxlaer, K.; Arana, B.; Mowbray, C. E.; Rafati, S.; Uliana, S.; Reguera, R.; Kreishman-Deitrick, M.; Sciotti, R.; Buffet, P.; Croft, S. L. Route map for the discovery and pre-clinical development of new drugs and treatments for cutaneous leishmaniasis. *Int. J. Parasitol.: Drugs Drug Resist.* **2019**, *11*, 106.

(27) Target product profile for cutaneous leishmaniasis: DNDi. https://dndi.org/diseases/cutaneous-leishmaniasis/target-product-profile/ (accessed June 25, 2021).

(28) Target product profile for visceral leishmaniasis: DNDi. https://dndi.org/diseases/visceral-leishmaniasis/target-product-profile/ (accessed June 25, 2021).

(29) Sundar, S.; Chakravarty, J. Antimony Toxicity. *Int. Res. J. Publ. Environ. Health* **2010**, *7*, 4267.

(30) Laurent, T.; Rijal, S.; Yardley, V.; Croft, S.; De Doncker, S.; Decuypere, S.; Khanal, B.; Singh, R.; Schönian, G.; Kuhls, K.; Chappuis, F.; Dujardin, J. C. Epidemiological dynamics of antimonial resistance in Leishmania donovani: genotyping reveals a polyclonal population structure among naturally-resistant clinical isolates from Nepal. *Infect. Genet. Evol.* **2007**, *7*, 206.

(31) Hefnawy, A.; Cantizani, J.; Peña, I.; Manzano, P.; Rijal, S.; Dujardin, J.-C.; De Muylder, G.; Martin, J. Importance of secondary screening with clinical isolates for anti-leishmania drug discovery. *Sci. Rep.* **2018**, *8*, 11765.

(32) Katsuno, K.; Burrows, J. N.; Duncan, K.; van Huijsduijnen, R. H.; Kaneko, T.; Kita, K.; Mowbray, C. E.; Schmatz, D.; Warner, P.; Slingsby, B. T. Hit and lead criteria in drug discovery for infectious diseases of the developing world. *Nat. Rev. Drug Discov.* **2015**, *14*, 751.

(33) Kratzerová, L.; Dráberová, E.; Juliano, C.; Viklický, V.; Fiori, P. L.; Cappuccinelli, P.; Dráber, P. Cell cycle-dependent changes in localization of a 210-kDa microtubule-interacting protein in Leishmania. *Exp. Cell Res.* **2001**, *266*, 270.

(34) Hernández, C.; Dunia, I.; Benedetti, E. L.; Dagger, F. Intermediate filament-like proteins in Leishmania. *Cell Biol. Int.* **1997**, *21*, 65.

(35) Burikhanov, R.; Sviripa, V. M.; Hebbar, N.; Zhang, W.; Layton, W. J.; Hamza, A.; Zhan, C.-G.; Watt, D. S.; Liu, C.; Rangnekar, V. M. Arylquins target vimentin to trigger Par-4 secretion for tumor cell apoptosis. *Nat. Chem. Biol.* **2014**, *10*, 924.

(36) Sviripa, V. M.; Burikhanov, R.; Obiero, J. M.; Yuan, Y.; Nickell, J. R.; Dwoskin, L. P.; Zhan, C.-G.; Liu, C.; Tsodikov, O. V.; Rangnekar, V. M.; Watt, D. S. Par-4 secretion: stoichiometry of 3-arylquinoline binding to vimentin. *Org. Biomol. Chem.* **2016**, *14*, 74.

(37) Ortiz, D.; Forquer, I.; Boitz, J.; Soysa, R.; Elya, C.; Fulwiler, A.; Nilsen, A.; Polley, T.; Riscoe, M. K.; Ullman, B.; Landfear, S. M. Targeting the Cytochrome bc1 Complex of Leishmania Parasites for Discovery of Novel Drugs. *Antimicrob. Agents Chemother.* **2016**, *60*, 4972.

(38) Zipper, H.; Brunner, H.; Bernhagen, J.; Vitzthum, F. Investigations on DNA intercalation and surface binding by SYBR Green I, its structure determination and methodological implications. *Nucleic Acids Res.* **2004**, *32*, No. e103.

(39) Marco-Contelles, J.; Pérez-Mayoral, E.; Samadi, A.; Carreiras, M. d. C.; Soriano, E. Recent advances in the Friedlander reaction. *Chem. Rev.* **2009**, *109*, 2652.

(40) Ritchie, T. J.; Macdonald, S. J. The impact of aromatic ring count on compound developability–are too many aromatic rings a liability in drug design? *Drug discovery today* **2009**, *14*, 1011.

(41) Tarcsay, A.; Nyíri, K.; Keserű, G. M. Impact of lipophilic efficiency on compound quality. *J. Med. Chem.* **2012**, *55*, 1252.

(42) Gleeson, M. P. Generation of a set of simple, interpretable ADMET rules of thumb. *J. Med. Chem.* **2008**, *51*, 817.

(43) Meanwell, N. A. Improving drug candidates by design: a focus on physicochemical properties as a means of improving compound disposition and safety. *Chem. Res. Toxicol.* **2011**, *24*, 1420.

(44) Lovering, F.; Bikker, J.; Humblet, C. Escape from flatland: increasing saturation as an approach to improving clinical success. *J. Med. Chem.* **2009**, *52*, 6752.

(45) Leeson, P. D.; Springthorpe, B. The influence of drug-like concepts on decision-making in medicinal chemistry. *Nat. Rev. Drug Discov.* **2007**, *6*, 881.

(46) Sacks, D. L. Animal models for the analysis of immune responses to leishmaniasis. *Curr. Protoc. Im.* **1998**, *19*, 19.2.